2007 IEEE International Conference on
Robotics and Automation
Roma, Italy, 10-14 April 2007

Proxy-Based Sliding Mode Control of a Manipulator Actuated by Pleated Pneumatic Artificial Muscles

M. Van Damme, B. Vanderborght, R. Van Ham, B. Verrelst, F. Daerden, D. Lefeber
Robotics and Multibody Mechanics Research Group
Department of Mechanical Engineering
Vrije Universiteit Brussel
Pleinlaan 2, 1050 Brussel
michael.vandamme@vub.ac.be

***Abstract*— Recently, Kikuuwe and Fujimoto have introduced Proxy-Based Sliding Mode Control. It combines responsive and accurate tracking during normal operation with smooth, slow recovery from large position errors that can sometimes occur after abnormal events. The method can be seen as an extension to both conventional PID control and sliding mode control.**

In this paper, Proxy-Based Sliding Mode Control is used to control a 2-DOF planar manipulator actuated by Pleated Pneumatic Artificial Muscles (PPAMs). The principal advantage of this control method is increased safety for people interacting with the manipulator.

Two different forms of Proxy-Based Sliding Mode Control were implemented on the system, and their performance was experimentally evaluated. Both forms performed very well with respect to safety. Good tracking was also obtained, especially with the second form.

I. Introduction

Manual material handling tasks such as lifting and carrying heavy loads, or maintaining static postures while supporting loads are a common cause of lower back disorders and other health problems. In fact, manual material handling has been associated with the majority of lower back injuries, which account for 16-19% of all workers compensation claims, while being responsible for 33-41% of all work-related compensations [1]. The problem has an important impact on the quality of life of affected workers, and it presents an important economic cost.

The traditional solution is using a commercially available manipulator system. Most of these systems use a counter-weight, which limits their use to handling loads of a specific mass.

In order to increase safety and productivity of human workers, several other approaches to robot-assisted manipulation have been studied in the robotics community [2], [3], [4]. The devices developed in the course of these studies belong to a class of materials handling equipment called Intelligent Assist Devices (IADs). Most of these systems, however, are heavy, complex and expensive.

We are working towards a multifunctional assistive device that can be used in direct interaction with a human operator, so safety is of paramount importance. As a first prototype, we have developed a small 2-DOF manipulator (shown in figure 1) powered by Pleated Pneumatic Artificial Muscles

Fig. 1. The manipulator. The series arrangement of Pleated Pneumatic Artificial Muscles is clearly visible.

(PPAMs, see [5]). The compliance of these actuators, combined with the very low total weight of the system ($\approx 2.6\,kg$) make the hardware intrinsically safe. It is essential, however, that the controller guarantees operator safety as well. This is why Proxy-Based Sliding Mode Control [6] is useful: it combines an overdamped, slow and safe recovery from unexpected disturbances and abnormal events with good tracking performance during normal operation. This is very difficult to achieve with for instance conventional PD or PID control: the high gains necessary to achieve accurate tracking also cause the system to accelerate violently (and dangerously) when its real and desired positions are far apart.

In this paper we present two different methods of implementing a Proxy-Based Sliding Mode controller for the 2-DOF pneumatic manipulator. The paper is organized as follows: section II gives an introduction to Proxy-Based Sliding Mode control, section III introduces the manipulator and section IV details the two implementations of Proxy-Based Sliding Mode Control, and provides experimental results obtained from tests on the manipulator. Conclusions are drawn in section V.

More information about the design of the manipulator can be found in [7].

II. Proxy-Based Sliding Mode Control

Proxy-Based Sliding Mode Control is a new control method that was introduced by Kikuuwe and Fujimoto in [6].

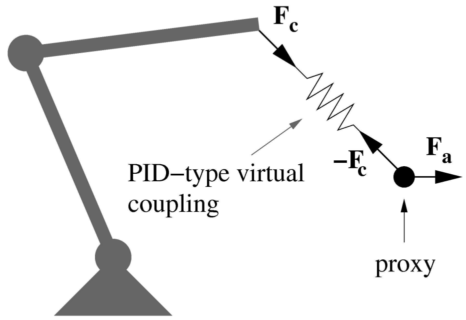

Fig. 2. Idea behind Proxy-Based Sliding Mode Control.

The basic idea behind Proxy-Based Sliding Mode Control for robotics is to attach an imaginary, virtual object, called proxy, to the robot's end effector by means of an imaginary, somewhat spring-like virtual coupling. This is illustrated in figure 2 for a 2-DOF robot in the horizontal plane. The proxy's trajectory is controlled by a sliding mode controller which exerts the force $\boldsymbol{F}_a$. Depending on their relative positions, the PID-type virtual coupling will cause an interaction force $\boldsymbol{F}_c$ between end effector and proxy. The (statical) torques that would be produced in the robot joints if $\boldsymbol{F}_c$ were physically present are given by the well-known relation

$$\boldsymbol{\tau} = J^T \boldsymbol{F}_c$$

(with J the the robot's Jacobian matrix). Actually applying these torques will cause the end effector's position to be servo-controlled to follow the proxy's position.

If $\boldsymbol{r}_p$ and $\dot{\boldsymbol{r}}_p$ are the proxy's position and velocity, and $\boldsymbol{r}_d$ and $\dot{\boldsymbol{r}}_d$ are the desired position and velocity, a sliding mode control law that can be used to control the proxy (initially modeled as a point mass) is given by

$$\boldsymbol{F}_a = F \operatorname{sgn}(\boldsymbol{s}) \tag{1}$$

with

$$\boldsymbol{s} = (\boldsymbol{r}_d - \boldsymbol{r}_p) + \lambda (\dot{\boldsymbol{r}}_d - \dot{\boldsymbol{r}}_p) \tag{2}$$

(see for instance [8] or [9] for an introduction to sliding mode control). Once the proxy has reached the sliding surface $s = 0$, its position and velocity errors will exponentially decay to zero, thus causing the proxy to gently converge to its desired trajectory.

The force produced by the PID-type virtual coupling is

$$\boldsymbol{F}_c = K_p (\boldsymbol{r}_p - \boldsymbol{r}) + K_i \int (\boldsymbol{r}_p - \boldsymbol{r})\, dt + K_d (\dot{\boldsymbol{r}}_p - \dot{\boldsymbol{r}}) \tag{3}$$

with $\boldsymbol{r}$ and $\dot{\boldsymbol{r}}$ the actual position and velocity, respectively. The equation of motion of the proxy is given by

$$m\ddot{\boldsymbol{r}}_p = \boldsymbol{F}_a - \boldsymbol{F}_c. \tag{4}$$

By introducing

$$\boldsymbol{a} = \int (\boldsymbol{r}_p - \boldsymbol{r})\, dt$$

and

$$\boldsymbol{\sigma} = (\boldsymbol{r}_d - \boldsymbol{r}) + \lambda (\dot{\boldsymbol{r}}_d - \dot{\boldsymbol{r}})$$

and using (2) equations (3) and (1) become

$$\boldsymbol{F}_c = K_p \dot{\boldsymbol{a}} + K_i \boldsymbol{a} + K_d \ddot{\boldsymbol{a}} \tag{5}$$

and

$$\boldsymbol{F}_a = \boldsymbol{F} \operatorname{sgn}(\boldsymbol{\sigma} - \dot{\boldsymbol{a}} - \lambda \ddot{\boldsymbol{a}}). \tag{6}$$

If we would want to implement a controller using (5) and (6), the motion of the proxy mass would have to be simulated in software. In [6], however, the proxy mass is set to zero. Equation (4) then gives us $\boldsymbol{F}_a = \boldsymbol{F}_c \equiv \boldsymbol{f}$, so we have the following equations:

$$\begin{aligned} \boldsymbol{\sigma} &= (\boldsymbol{r}_d - \boldsymbol{r}) + \lambda (\dot{\boldsymbol{r}}_d - \dot{\boldsymbol{r}}) && (7) \\ \boldsymbol{f} &= F \operatorname{sgn}(\boldsymbol{\sigma} - \dot{\boldsymbol{a}} - \lambda \ddot{\boldsymbol{a}}) && (8) \\ \boldsymbol{f} &= K_p \dot{\boldsymbol{a}} + K_i \boldsymbol{a} + K_d \ddot{\boldsymbol{a}} && (9) \end{aligned}$$

By discretizing equations (7)-(9) and solving the resulting equations for the unknowns $\boldsymbol{a}$ and $\boldsymbol{f}$, Kikuuwe and Fujimoto [6] derive a discrete time controller that satisfies (7)-(9), the so-called Proxy-Based Sliding Mode controller. The value of $\boldsymbol{f}$ at timestep k can be calculated by the following computational procedure [6]:

$$\begin{aligned} \boldsymbol{\sigma}(k) &= (\boldsymbol{r}_d(k) - \boldsymbol{r}(k)) + \lambda (\dot{\boldsymbol{r}}_d(k) - \dot{\boldsymbol{r}}(k)) && (10) \\ \boldsymbol{f}^*(k) &= \frac{K_d + K_p T + K_i T^2}{\lambda + T} \boldsymbol{\sigma}(k) + K_i \boldsymbol{a}(k-1) \\ &\quad + \frac{(K_p + K_i T)\lambda - K_d}{(\lambda + T) T} \nabla \boldsymbol{a}(k-1) && (11) \\ \boldsymbol{f}(k) &= \begin{cases} \boldsymbol{f}^*(k) & \text{if } \|\boldsymbol{f}^*(k)\| \leq F \\ F \boldsymbol{f}^*(k) / \|\boldsymbol{f}^*(k)\| & \text{if } \|\boldsymbol{f}^*(k)\| > F \end{cases} && (12) \\ \boldsymbol{a}(k) &= \frac{1}{K_d + K_p T + K_i T^2} \big((K_d + K_p T)\, \boldsymbol{a}(k-1) \\ &\quad + K_d \nabla \boldsymbol{a}(k-1) + T^2 \boldsymbol{f}(k) \big) && (13) \end{aligned}$$

In these equations, T is the sampling period and ∇ is the backward difference operator, defined as $\nabla x(k) = x(k) - x(k-1)$.

By setting $\lambda = 0$ and $F \to \infty$, equations (10)-(13) become equivalent to a discrete-time PID controller. With $K_i = 0$ and $\lambda = K_d/K_p$ they can be seen as force-limited PID control, or as sliding mode control with a boundary layer. Proxy-Based Sliding Mode Control can thus be seen as an extension of these conventional methods.

The main advantage of the method is the separation of "local" and "global" dynamics. The local dynamics, i.e. the response to small positional errors, is determined by the virtual coupling (parameters K_p, K_i and K_d), while the global dynamics (response to large positional errors) is determined by the sliding mode parameter λ. It is thus possible to combine responsive and accurate tracking during normal operation with smooth, slow and safe recovery from large position errors that can sometimes occur after abnormal events.

III. Manipulator

A. Introduction

Since the developed manipulator is a first prototype, the length of both links was kept small: 30 cm. Figure 3 shows

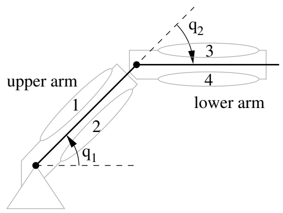

Fig. 3. The inverse elbow configuration.

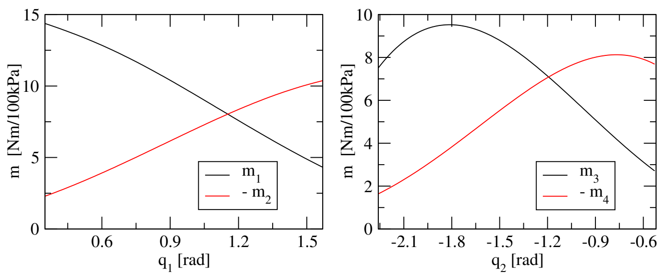

Fig. 4. Torque functions.

the conventions used in the rest of this document regarding to how both joint angles are defined and how the different pneumatic muscles are numbered.

B. Torque characteristics

From the knowledge of the system's kinematic parameters (i.e. muscle attachment point locations) and the PPAM actuator parameters, we can determine the torque characteristics of both joints. Using the nonlinear force-pressure-contraction relation of the PPAM muscle (see [5], [10]), the torque generated by a muscle can be written as

$$\tau_{m,i} = p \cdot m_i(\gamma) \tag{14}$$

with $\gamma = q_1$ for muscles 1 and 2 and $\gamma = q_2$ for muscles 3 and 4. The total actuator torque (in both joints) can thus be represented by

$$\boldsymbol{\tau} = \begin{bmatrix} \tau_{m,1} + \tau_{m,2} \\ \tau_{m,3} + \tau_{m,4} \end{bmatrix} = \begin{bmatrix} p_1 \cdot m_1(q_1) + p_2 \cdot m_2(q_1) \\ p_3 \cdot m_3(q_2) + p_4 \cdot m_4(q_2) \end{bmatrix}. \tag{15}$$

Equation (14) provides a clear separation between the two factors that determine torque: gauge pressure and a torque function $m_i(\gamma)$, that depends on the design parameters and the position. The torque functions m_i are shown in figure 4. More details can be found in [7]. Note however, that these torque functions provide a relatively rough approximation of reality.

IV. Control

A. Introduction

In general, controlling the manipulator is not straightforward. Difficulties encountered when designing a controller include the following:

- Non-linear force-contraction relation of the PPAM actuator (see [5], [10]).
- Hysteresis in the force-contraction relation of the PPAM. Although the hysteresis effect is less pronounced in the PPAM than in other types of pneumatic artificial muscles, it still makes it difficult to estimate the actual force exerted by the actuator.
- Imprecise knowledge of PPAM parameters.
- Non-linearity in the pressure regulating valves.
- Actuator gauge pressures can take a relatively long time to settle (around 100 ms for large pressure steps).
- The coupling between actuator gauge pressures and link angles and angular velocities. This means that the system cannot be modeled as a cascade of a pneumatic system followed by a mechanical system.

These factors have made it a difficult task to efficiently control the system, especially since overall system safety is a very important factor as well. Proxy-Based Sliding Mode, however, turns out to perform well, while being very safe for operators to interact with the system.

B. Δp - approach

To reduce the number of actuator outputs that have to be calculated, the Δp-approach was used (see [10], [11]). This involves choosing an average pressure p_m for both muscles of an antagonistic pair, and having the controller calculate a pressure difference Δp that is added in one muscle $(p + \Delta p)$ and subtracted in the other $(p - \Delta p)$. The choice of p_m influences compliance while Δp determines joint position.

The control of the actuator pressures themselves is handled by off-the-shelf proportional pressure regulating valves with internal PID controllers.

C. Proxy-Based Sliding Mode Control - First method

We started by implementing the Proxy-Based Sliding Mode controller as described in [6], but with the addition of a gravity compensation term:

$$\boldsymbol{\tau}(k) = \boldsymbol{\tau}_{gc}(k) + \boldsymbol{\tau}_{pbsm}(k)$$

$\boldsymbol{\tau}_{gc}(k)$ is the torque needed for static gravity compensation, while $\boldsymbol{\tau}_{pbsm}(k)$ is the torque calculated by the Proxy-Based Sliding Mode controller:

$$\boldsymbol{\tau}_{pbsm}(k) = J^T \boldsymbol{f}(k),$$

with $\boldsymbol{f}(k)$ calculated from equations (10)-(13).

In order to apply this torque, we have to know the corresponding actuator gauge pressures. We can calculate them by rewriting (15) in view of the Δp - approach ($p_{2i-1} = p_m + \Delta p_i$ and $p_{2i} = p_m - \Delta p_i$ for $i = 1, 2$):

$$\boldsymbol{\tau} = \begin{bmatrix} p_m\left(m_1(q_1) + m_2(q_1)\right) + \Delta p_1\left(m_1(q_1) - m_2(q_1)\right) \\ p_m\left(m_3(q_2) + m_4(q_2)\right) + \Delta p_2\left(m_3(q_2) - m_4(q_2)\right) \end{bmatrix}$$

so we have

$$\begin{bmatrix} \Delta p_1(k) \\ \Delta p_2(k) \end{bmatrix} = \begin{bmatrix} \frac{\tau_1(k) - p_m(m_1(q_1)+m_2(q_1))}{m_1(q_1)-m_2(q_1)} \\ \frac{\tau_2(k) - p_m(m_3(q_2)+m_4(q_2))}{m_3(q_2)-m_4(q_2)} \end{bmatrix} \tag{16}$$

with $\boldsymbol{\tau} = \begin{bmatrix} \tau_1(k) & \tau_2(k) \end{bmatrix}^T$.

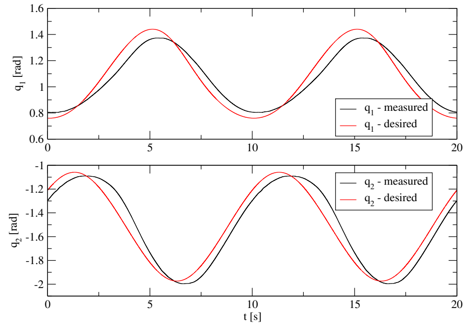

Fig. 5. Measured and desired joint angles while tracking a circular trajectory (period $= 10s$).

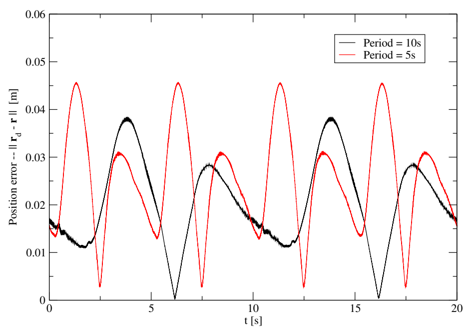

Fig. 6. Position errors for tracking circular trajectories with periods of 10 and 5 seconds.

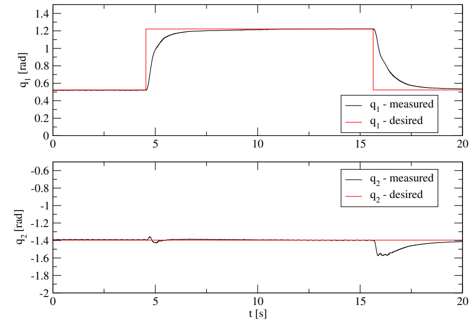

Fig. 7. System response to a step change in desired angle values.

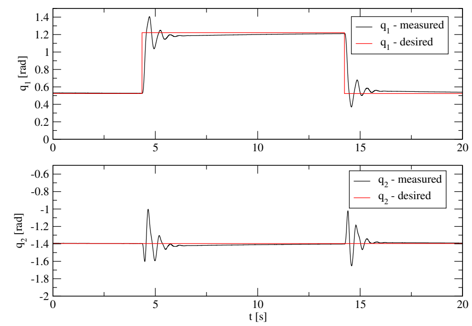

Fig. 8. System response to a step change in desired angle values when using a PID + gravity compensation controller. Note the difference with the response from the Proxy-Based Sliding Mode controller (see fig. 7).

D. Experimental Results

The first experiment we performed was having the manipulator track a circular trajectory with a diameter of $20\,cm$. The results are shown in fig. 5 for a circle-period of 10 seconds (10 seconds per revolution). The positional error $\|\boldsymbol{r}_d - \boldsymbol{r}\|$ (with $\boldsymbol{r}$ the cartesian position and $\boldsymbol{r}_d$ the desired cartesian position) is shown in figure 6. Tracking precision isn't great, but for this hard to control system the performance is certainly comparable to results obtained with other controllers. As can be expected, figure 6 clearly shows that position errors increase with desired angular velocities.

When evaluating tracking performance, we found that relatively accurate estimates of the system parameters were essential in order to achieve acceptable results, much more so than in the second method described below (see section IV-E). The system parameters are used for gravity compensation and for converting between torques and pressures (see equation (16)). An inaccurate model leads to severe degradation of tracking performance.

We also tested the response to input steps as shown in figure 7, where the desired value for q_1 is switched between $30\pi/180$ and $70\pi/180$ while the desired value for q_2 is kept constant at $-80\pi/180$. The smooth, overdamped response is clearly visible.

For comparison, the violent response and overshoot we get form a PID + gravity compensation controller when applying a similar input step is shown in figure 8. Lowering the PID gains will cause a more gradual response, but tracking performance then becomes very bad. The Proxy-Based Sliding Mode controller is obviously safer when dealing with large input steps, while still providing acceptable tracking performance.

In order to further test the safety aspects, we switched the desired trajectory discontinuously between two circular paths. The original circular trajectory had a period of 3.333 seconds, while the second had a period of 10 seconds. The result is shown in figure 9. It is clear that the transition is smooth, overdamped and safe for the operator.

In a final safety related test, we set a fixed target position and observed the manipulator's behaviour when it was manually pushed to random positions and then released. The system's behaviour is shown in figure 10. It was easy to push

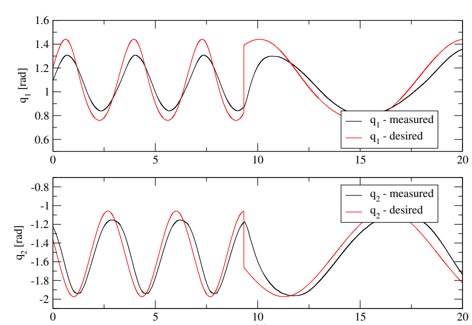

Fig. 9. System response to discontinuous change in desired trajectory.

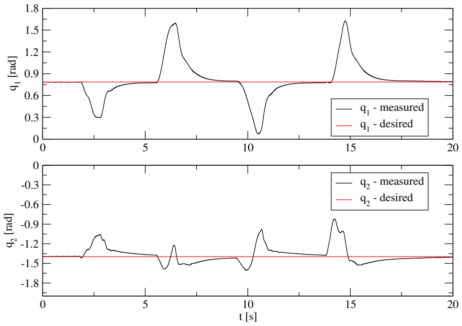

Fig. 10. The system's behaviour when it is repeatedly pushed away from its target position and then released.

TABLE I

PARAMETER VALUES

Parameter	Value
$\lambda\ (s)$	0.4
$K_p\ (N/m)$	200
$K_i\ (N/ms)$	100
$K_d\ (Ns/m)$	10
$F\ (N)$	10

(a) First method

Links 1 and 2	
Parameter	Value
$\lambda\ (s)$	0.4
$K_p\ (bar/rad)$	2
$K_i\ (bar/rad \cdot s)$	2
$K_d\ (bar \cdot s/rad)$	0.1
$\Delta p_{lm}\ (bar)$	0.2

(b) Second method

the system away from its target position, and it recovered smoothly when it was released.

The parameter values used in the controller during the experiments are shown in table I (first method).

E. Proxy-Based Sliding Mode Control – Second method

Since the tracking performance obtained using the previously described controller wasn't entirely satisfactory, we have implemented Proxy-Based Sliding Mode control by interpreting it in a different way, which results in a controller less sensitive to model inaccuracies.

In this second form of Proxy-Based Sliding Mode control, we control both links separately. Consider a single robot link in the horizontal plane, as shown in fig. 11. In this case, we consider the proxy to be a virtual link attached to the real link by means of a torsional PID-type virtual coupling. Since the proxy's equation of motion is given by

$$I\ddot{q}_p = \tau_a - \tau_c$$

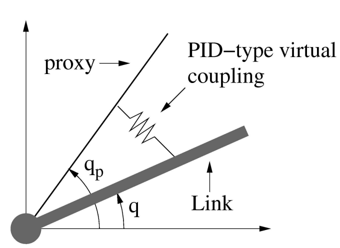

Fig. 11. Proxy-Based Sliding Mode Control - Second Method

with

$$\tau_a = \tau_{lm}\,\mathrm{sgn}\left((q_d - q_p) + \lambda\left(\dot{q}_d - \dot{q}_p\right)\right)$$
$$\tau_c = K_p\left(q_p - q\right) + K_i \int \left(q_p - q\right) dt + K_d\left(\dot{q}_p - \dot{q}\right)$$

we arrive at

$$\tau = \tau_{lm}\,\mathrm{sgn}\left(\sigma - \dot{a} - \lambda\ddot{a}\right) \quad (17)$$
$$\tau = K_p\dot{a} + K_i a + K_d\ddot{a} \quad (18)$$

by setting $a = \int (q_p - q)\,dt$, $\sigma = (q_d - q) + \lambda\left(\dot{q}_d - \dot{q}\right)$ and $I = 0$, exactly as in section II. Since equations (17)-(18) are simply a one-dimensional form of (7)-(9) (although angles are used instead of cartesian coordinates), we can reuse Kikuuwe and Fujimoto's discrete-time solution [6].

In the case of the pneumatic manipulator we want to control, it is more appropriate to work directly with values of Δp instead of using torques, since we are using the pressure difference to set the torque anyway. Having the controller output values of Δp directly effectively bypasses the angle-dependent torque to Δp conversion that was necessary in the first method. The Proxy-Based Sliding mode control law now becomes

$$\sigma = (q_d - q) + \lambda\left(\dot{q}_d - \dot{q}\right) \quad (19)$$
$$\Delta p_p^*(k) = \frac{K_d + K_pT + K_iT^2}{\lambda + T}\sigma(k) + K_i a(k-1) + \frac{(K_p + K_iT)\,\lambda - K_d}{(\lambda + T)\,T}\nabla a(k-1) \quad (20)$$
$$\Delta p_p(k) = \begin{cases} \Delta p_p^*(k) & \text{if } \left|\Delta p_p^*(k)\right| \leq \Delta p_{lm} \\ \Delta p_{lm}\,\mathrm{sgn}\left(\Delta p_p^*(k)\right) & \text{if } \left|\Delta p_p^*(k)\right| > \Delta p_{lm} \end{cases} \quad (21)$$
$$a(k) = \frac{1}{K_d + K_pT + K_iT^2}\left(\left(K_d + K_pT\right)a(k-1) + K_d\nabla a(k-1) + T^2\Delta p_p(k)\right). \quad (22)$$

Δp_{lm} is a pressure limit similar to the force limit F in equations (10)-(13).

Since the manipulator works in the vertical plane, gravity compensation has to be added. The control law thus becomes

$$\Delta p(k) = \Delta p_{gc}(k) + \Delta p_p(k), \quad (23)$$

with $\Delta p_p(k)$ calculated from (19)-(22) and $\Delta p_{gc}(k)$ the Δp value necessary for static gravity compensation. Of course, the accuracy of $\Delta p_{gc}(k)$ still depends on how accurate the model used for the actuators and the manipulator is.

Both links are separately controlled using control law (23).

F. Experimental results – Second method

For comparison, we performed the same experiments with the second control method as with the first (see section IV-D). The results are shown in figures 12, 13, 14, 15 and 16.

It is obvious from figures 12 and 13 that tracking performance is much better than in the previous case. For a pneumatic system, this can be considered as very good tracking.

Safety (i.e. slow and smooth response to big steps and a smooth recovery to disturbances), is just as good as with the first method.

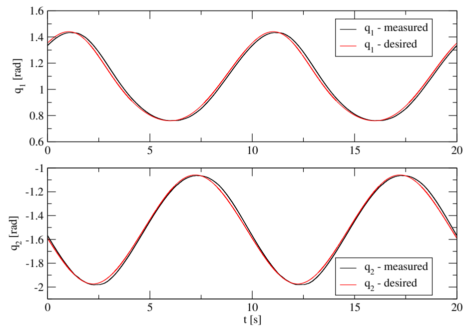

Fig. 12. Measured and desired joint angles while tracking a circular trajectory using the second control method (period $= 10s$).

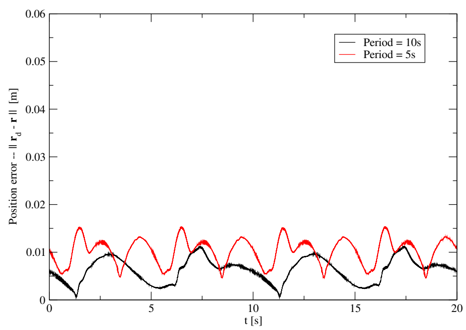

Fig. 13. Position errors for tracking circular trajectories with periods of 10 and 5 seconds using control method 2. For easy comparison, the same scale was used as in fig. 6.

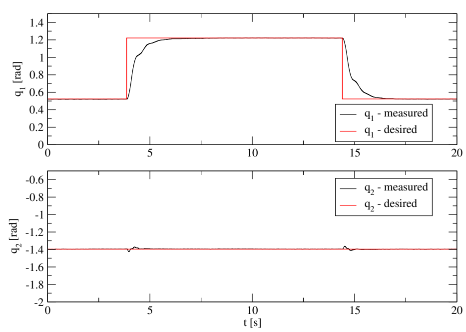

Fig. 14. System response to a step change in desired angle values (second control method).

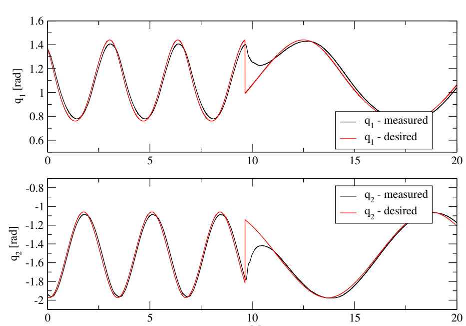

Fig. 15. System response to discontinuous change in desired trajectory (second control method).

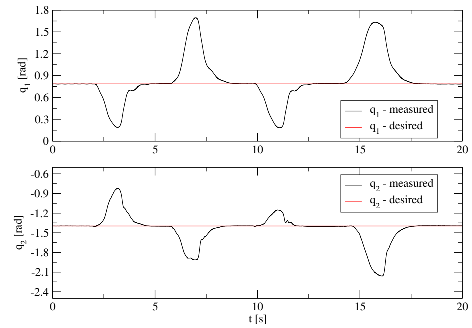

Fig. 16. The system's behaviour when it is repeatedly pushed away from its target position and then released (second control method).

V. Conclusions

This paper describes an application of the Proxy-Based Sliding Mode Control method, introduced by Kikuuwe and Fujimoto in [6], to the control of a planar 2-DOF manipulator actuated by Pleated Pneumatic Artificial Muscles. Two ways of implementing Proxy-Based Sliding Mode Control were implemented and tested, and experimental results were provided. Good tracking performance was obtained, especially with the second control method. Performance with respect to safety, crucial for this system, is very good.

Acknowledgements

This work is supported by the Fund for Scientific Research (FWO) - Flanders (Belgium) and by the Research Council (OZR) of the Vrije Universiteit Brussel.

References

[1] W.S. Marras, K.P. Granata, K.G. Davis, W.G. Allread, and M.J. Jorgensen, "Effects of box features on spine loading during warehouse order selecting," *Ergonomics*, vol. 42, no. 7, pp. 980–996, 1999.

[2] Kevin M. Lynch and Caizhen Liu, "Designing Motion Guides for Ergonomic Collaborative Manipulation," *IEEE International Conference on Robotics and Automation*, 2000.

[3] H. Kazerooni, "The human power amplifier technology at the University of California, Berkeley," *Journal of Robotics and Autonomous Systems*, vol. 19, pp. 179–187, 1996.

[4] Jae H. Chung, "Control of an operator-assisted mobile robotic system," *Robotica*, vol. 20, no. 4, pp. 439–446, 2002.

[5] Daerden F. and Lefeber D., "The concept and design of pleated pneumatic artificial muscles," *International Journal of Fluid Power*, vol. 2, no. 3, pp. 41–50, 2001.

[6] R. Kikuuwe and H. Fujimoto, "Proxy-based sliding mode control for accurate and safe position control," in *Proceedings of the 2006 IEEE International conference on Robotics and Automation*, 2006, pp. 25–30.

[7] Van Damme M., Daerden F., and Lefeber D., "A pneumatic manipulator used in direct contact with an operator," in *Proceedings of the 2005 IEEE International Conference on Robotics and Automation*, Barcelona, Spain, April 2005, pp. 4505–4510.

[8] J.-J. Slotine and W. Li, *Applied Nonlinear Control*. Prentice Hall, 1991.

[9] John Y. Hung, Weibing Gao, and James C. Hung, "Variable structure control: A survey," *IEEE Tranasctions on Industrial Electronics*, vol. 40, no. 1, pp. 2–22, 1993.

[10] Frank Daerden, "Conception and Realization of Pleated Pneumatic Artificial Muscles and their Use as Compliant Actuation Elements," Ph.D. dissertation, Vrije Universiteit Brussel, 1999.

[11] Daerden F., Lefeber D., Verrelst B., and Van Ham R., "Pleated pneumatic artificial muscles: actuators for automation and robotics"," in *IEEE/ASME International Conference on Advanced Intelligent Mechatronics*, Como, Italy, July 2001, pp. 738–743.